

GL-TR-90-0027

AD-A223 229

Electrodynamics of the High Latitude Ionosphere

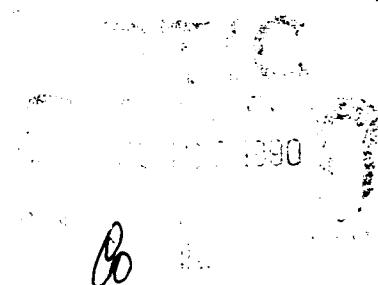
R. A. Heelis

University of Texas at Dallas
Center for Space Sciences
P. O. Box 830688
Richardson, TX 75083-0688

February 1990

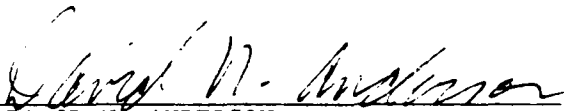
Final Report
September 1986-September 1989

APPROVED FOR PUBLIC RELEASE; DISTRIBUTION UNLIMITED

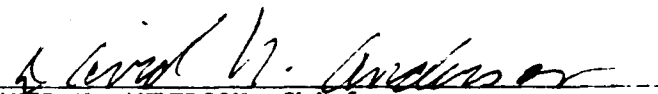


GEOPHYSICS LABORATORY
AIR FORCE SYSTEMS COMMAND
UNITED STATES AIR FORCE
HANSCOM AIR FORCE BASE, MASSACHUSETTS 01731-5000

"This technical report has been reviewed and is approved for publication"



DAVID N. ANDERSON
Contract Manager



DAVID N. ANDERSON, Chief
Ionospheric Modelling & Remote Sensing Branch
Ionospheric Physics Division

FOR THE COMMANDER



ROBERT A. SKRIVANEK, Director
Ionospheric Physics Division

Qualified requestors may obtain additional copies from the Defense Technical Information Center. All others should apply to the National Technical Information Service (NTIS).

If your address has changed, or if you wish to be removed from the mailing list, or if the addressee is no longer employed by your organization, please notify GL/IMA, Hanscom AFB, MA. 01731. This will assist us in maintaining a current mailing list.

Do not return copies of this report unless contractual obligations or notices on a specific document requires that it be returned.

REPORT DOCUMENTATION PAGE			Form Approved OMB No. 0704-0188	
<small>Supplied by the Government of the United States of America. Information is not to be released to the public without the approval of the Department of Defense. The Department of Defense is not responsible for the collection, use, or dissemination of information. Send comments regarding this burden estimate or any other aspect of this form, including suggestions for reducing this burden, to Washington Headquarters Services, Directorate for Information Operations and Reports, 1215 Jefferson Avenue, Suite 1204, Washington, DC 22202-4302, and to the Office of Management and Budget, Paperwork Reduction Project (0704-0188), Washington, DC 20503.</small>				
1. AGENCY USE ONLY (Leave blank)		2. REPORT DATE February 1990	3. REPORT TYPE AND DATES COVERED Final Report Sept. 1986 - Sept. 1989	
4. TITLE AND SUBTITLE Electrodynamics of the High Latitude Ionosphere			5. FUNDING NUMBERS PE: 61102F PR 2310 TAG9 WUAD	
6. AUTHOR(S) R. A. Heelis			Contract F19628-86-K-0042	
7. PERFORMING ORGANIZATION NAME(S) AND ADDRESS(ES) University of Texas at Dallas Center for Space Sciences P. O. Box 830688 Richardson, TX 75083-0688			8. PERFORMING ORGANIZATION REPORT NUMBER	
9. SPONSORING / MONITORING AGENCY NAME(S) AND ADDRESS(ES) Geophysics Laboratory Hanscom AFG, Massachusetts 01731-5000 Contract Manager: David Anderson/LIM			10. SPONSORING MONITORING AGENCY REPORT NUMBER GL-TR-90-0027	
11. SUPPLEMENTARY NOTES				
12a. DISTRIBUTION AVAILABILITY STATEMENT Approved for public release; distribution unlimited			12b. DISTRIBUTION CODE	
13. ABSTRACT (Maximum 200 words) Both large and small scale structure in the plasma density and velocity are important phenomena to be understood in the ionosphere. The ability to characterize the high-latitude plasma motion over large spatial scales is demonstrated here with the development of a model that can be driven by data inputs. The model can also be used to study the mechanisms producing large scale structures in the plasma. The applicability of the model is demonstrated for periods when the interplanetary magnetic field has a southward component. During periods of northward IMF the electrodynamics of the ionosphere on spatial scales of 100 km must be understood. Here the combination of ground based and space based data are invaluable tools. We show that mesoscale features may be coherent over many hours and constitute an important signature of the interaction of the Earth's magnetic field with the interplanetary medium.				
14. SUBJECT TERMS Ionosphere, Plasma, Electric Fields			15. NUMBER OF PAGES 34	
			16. PRICE CODE	
17. SECURITY CLASSIFICATION OF REPORT Unclassified	18. SECURITY CLASSIFICATION OF THIS PAGE Unclassified	19. SECURITY CLASSIFICATION OF ABSTRACT Unclassified	20. LIMITATION OF ABSTRACT SAR	

CONTENTS

	PAGE
1. Introduction	1
2. Ionospheric Electrodynamics	2
2.1 A Model of the High Latitude Convection Pattern	2
2.1.1 Southward IMF	3
2.1.2 Northward IMF	6
2.1.3 Temporal Evolution of the Convection Pattern	10
2.2 Plasma Structures and Convective Flow	12
2.3 Electrodynamics of Polar Cap Arcs	13
2.4 Electrical Coupling in Ionospheric Structures	17
3. Ionospheric Frictional Heating	19
References	22
4. Publications	24

Accession For
1973
1974
1975
1976
1977
1978
1979
1980
1981
1982
1983
1984
1985
1986
1987
1988
1989
1990
1991
1992
1993
1994
1995
1996
1997
1998
1999
2000
2001
2002
2003
2004
2005
2006
2007
2008
2009
2010
2011
2012
2013
2014
2015
2016
2017
2018
2019
2020
2021
2022
2023
2024
2025
2026
2027
2028
2029
2030
2031
2032
2033
2034
2035
2036
2037
2038
2039
2040
2041
2042
2043
2044
2045
2046
2047
2048
2049
2050
2051
2052
2053
2054
2055
2056
2057
2058
2059
2060
2061
2062
2063
2064
2065
2066
2067
2068
2069
2070
2071
2072
2073
2074
2075
2076
2077
2078
2079
2080
2081
2082
2083
2084
2085
2086
2087
2088
2089
2090
2091
2092
2093
2094
2095
2096
2097
2098
2099
2100
2101
2102
2103
2104
2105
2106
2107
2108
2109
2110
2111
2112
2113
2114
2115
2116
2117
2118
2119
2120
2121
2122
2123
2124
2125
2126
2127
2128
2129
2130
2131
2132
2133
2134
2135
2136
2137
2138
2139
2140
2141
2142
2143
2144
2145
2146
2147
2148
2149
2150
2151
2152
2153
2154
2155
2156
2157
2158
2159
2160
2161
2162
2163
2164
2165
2166
2167
2168
2169
2170
2171
2172
2173
2174
2175
2176
2177
2178
2179
2180
2181
2182
2183
2184
2185
2186
2187
2188
2189
2190
2191
2192
2193
2194
2195
2196
2197
2198
2199
2200
2201
2202
2203
2204
2205
2206
2207
2208
2209
2210
2211
2212
2213
2214
2215
2216
2217
2218
2219
2220
2221
2222
2223
2224
2225
2226
2227
2228
2229
2230
2231
2232
2233
2234
2235
2236
2237
2238
2239
2240
2241
2242
2243
2244
2245
2246
2247
2248
2249
2250
2251
2252
2253
2254
2255
2256
2257
2258
2259
2260
2261
2262
2263
2264
2265
2266
2267
2268
2269
2270
2271
2272
2273
2274
2275
2276
2277
2278
2279
2280
2281
2282
2283
2284
2285
2286
2287
2288
2289
2290
2291
2292
2293
2294
2295
2296
2297
2298
2299
2300
2301
2302
2303
2304
2305
2306
2307
2308
2309
2310
2311
2312
2313
2314
2315
2316
2317
2318
2319
2320
2321
2322
2323
2324
2325
2326
2327
2328
2329
2330
2331
2332
2333
2334
2335
2336
2337
2338
2339
2340
2341
2342
2343
2344
2345
2346
2347
2348
2349
2350
2351
2352
2353
2354
2355
2356
2357
2358
2359
2360
2361
2362
2363
2364
2365
2366
2367
2368
2369
2370
2371
2372
2373
2374
2375
2376
2377
2378
2379
2380
2381
2382
2383
2384
2385
2386
2387
2388
2389
2390
2391
2392
2393
2394
2395
2396
2397
2398
2399
2400
2401
2402
2403
2404
2405
2406
2407
2408
2409
2410
2411
2412
2413
2414
2415
2416
2417
2418
2419
2420
2421
2422
2423
2424
2425
2426
2427
2428
2429
2430
2431
2432
2433
2434
2435
2436
2437
2438
2439
2440
2441
2442
2443
2444
2445
2446
2447
2448
2449
2450
2451
2452
2453
2454
2455
2456
2457
2458
2459
2460
2461
2462
2463
2464
2465
2466
2467
2468
2469
2470
2471
2472
2473
2474
2475
2476
2477
2478
2479
2480
2481
2482
2483
2484
2485
2486
2487
2488
2489
2490
2491
2492
2493
2494
2495
2496
2497
2498
2499
2500
2501
2502
2503
2504
2505
2506
2507
2508
2509
2510
2511
2512
2513
2514
2515
2516
2517
2518
2519
2520
2521
2522
2523
2524
2525
2526
2527
2528
2529
2530
2531
2532
2533
2534
2535
2536
2537
2538
2539
2540
2541
2542
2543
2544
2545
2546
2547
2548
2549
2550
2551
2552
2553
2554
2555
2556
2557
2558
2559
2560
2561
2562
2563
2564
2565
2566
2567
2568
2569
2570
2571
2572
2573
2574
2575
2576
2577
2578
2579
2580
2581
2582
2583
2584
2585
2586
2587
2588
2589
2590
2591
2592
2593
2594
2595
2596
2597
2598
2599
2600
2601
2602
2603
2604
2605
2606
2607
2608
2609
2610
2611
2612
2613
2614
2615
2616
2617
2618
2619
2620
2621
2622
2623
2624
2625
2626
2627
2628
2629
2630
2631
2632
2633
2634
2635
2636
2637
2638
2639
2640
2641
2642
2643
2644
2645
2646
2647
2648
2649
2650
2651
2652
2653
265



ELECTRODYNAMICS OF THE HIGH LATITUDE IONOSPHERE

1. Introduction.

The study of high latitude ionospheric electrodynamics is important to both our understanding of the ionospheric plasma and to an understanding of the interaction between the Earth's magnetic field with the interplanetary medium. A quantitative description of the convective motion of the high latitude ionospheric plasma is being pursued for the purpose of studying plasma structures where the convective history of the plasma may be important. The model developed for describing conditions during southward interplanetary magnetic field (IMF) has been adapted to possess a flexibility allowing some representations of convection patterns that may exist during times of northward IMF. Of particular interest during times of northward IMF is the electric field configuration associated with stable auroral features at very high latitudes. The electrodynamic configuration of these features has been described using a variety of satellite and ground based diagnostics that may also help us to understand the global configuration of the magnetic and the electric field associated with them.

The dominance of small-scale structure in the electric field and plasma density during times of northward IMF has lead to a study of the ways in which these parameters are coupled. While it is customary to think of the Earth's magnetic field lines as electric equipotentials, it can be shown that they are far from exhibiting this property for scale sizes less than a few kilometers. The effects that scale-size dependent electric field mapping has on the development of plasma structure has been investigated in some detail. Large and small scale electric fields in the ionosphere drive horizontal currents that are ohmically dissipated as heat in the altitude region below about 250 km.. Above this altitude significant frictional heating of the ions can occur as a result of a relative drift between the ions and the neutral gas. We have studied the differences between representations of this heating in terms of a height-integrated Joule heating rate and an in-situ frictional heating rate. It can be quite clearly seen that the heating rate per particle must be considered in each region of interest in order to relate measurements made in one region to conditions existing in another.

The research activities reported on here, represent some significant advances in our understanding of physical processes in the high latitude ionosphere. They also provide some tools with which the phenomena can be modelled and represented. The work described

here has significant implications for future efforts and points to the need to consider, not only the high latitude region but also the degree to which the electrodynamics is coupled to low and mid-latitudes.

2. Ionospheric Electrodynamics.

Here we describe the results of studies of large-scale (> 50 km.) electric fields in the ionosphere from a source, or sources, in the outer magnetosphere. We attempt to describe the configuration of these fields in the ionosphere, their dependence on the orientation of the IMF, and the magnetic and electric field configuration in the magnetosphere with which they may be consistent. In addition to externally applied electric fields, we also consider the internal generation of much smaller-scale electric fields produced by plasma structures. In this case, the process of electrical coupling between different regions of the ionosphere must be considered in some detail, since the magnetic field lines may not be regarded as electric equipotentials.

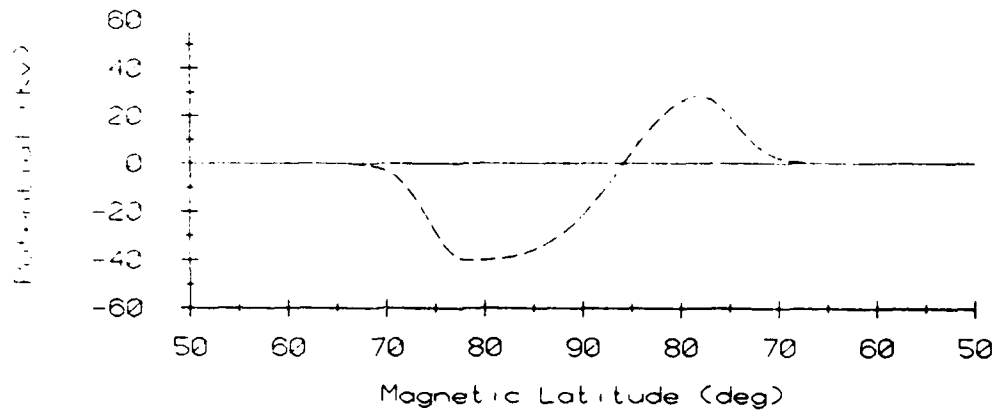
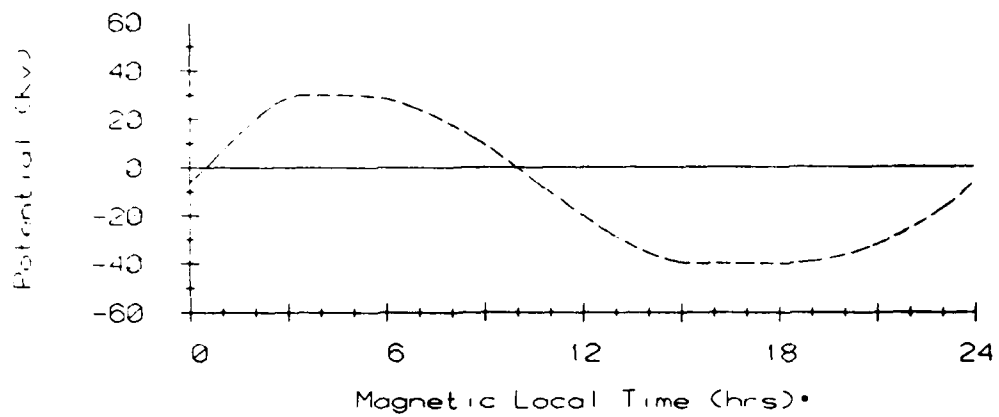
2.1. A model of the High Latitude Convection Pattern.

Many studies of the high latitude convection pattern have shown that temporal changes in the configuration of the pattern and the magnitude of the electric potential are extremely important considerations (Lockwood and Cowley, 1988). While measurements of the convective properties may be dominated by these effects the desire to be able to instantaneously describe the convective motion of the plasma still exists from the point of view of determining the effects of convective history on the composition and total concentration of the ionospheric plasma. Ultimately we would like to determine all the parameters affecting the configuration of the high latitude convection pattern and specify a model, dependent on these parameters. While we are not yet in this position, we have advanced to a stage where analytical expressions can be used to represent the large scale properties of the convection pattern for southward IMF. These expressions allow convective cells of different geometries to be constructed and can therefore simulate the major features of an IMF B_y dependence for the case when the IMF has a southward component and distorted two-cell convection patterns when the IMF has a northward component. In addition to developing the mathematical expressions themselves, we have also examined our capability to reproduce a given satellite observation. In this area we have studied the high latitude potential distribution obtained from specifying only the potential distribution around the convection reversal boundary, and the shape of the boundary. Specific developments are summarized below.

2.1.1. Southward IMF

When the IMF has a southward component the high latitude ionospheric convection pattern is characterized two counter-rotating vortices producing antisunward convection at highest latitudes and sunward convection at lower latitudes. A representation of the convective motion of the plasma is obtained by illustrating lines of constant electric potential, along which, in steady state, the plasma must flow. The major attributes of these electric potential streamlines that make up the convection cells are their geometrical size and shape and the absolute value of the potential extrema that is represented by them. We have found that the convection pattern can be characterized very broadly by a circular region inside which the plasma flow is antisunward and beyond which the magnitude of the potential decreases with latitude. A quantitative description of the convection pattern can be obtained by specifying the local time distribution of the potential around the boundary of the circular region and the latitude distribution of the potential along a local time meridian. We will call the boundary of the circular region, the convection reversal boundary. Figure 1 shows a representation of the convection pattern derived from the information given above. Lines of constant potential are shown to represent the convection streamlines. The latitude distribution of potential along the 0600-1800 meridian and the distribution around the convection reversal boundary, assumed to be a circle of radius 12° , are also shown. This formulation allows the relative shape of the convection cells to be changed by changing these two distributions. Figure 2 shows two representations of the convection pattern that can be produced by changing these two distributions. They can be used to approximate empirical representations of the pattern for positive and negative values of IMF B_y respectively. We note that the changes in the shape of the pattern are obtained by moving the location of the zero potential line on the dawn-dusk meridian and by changing the local time distribution of the potential. Thus a more quantitative representation of the pattern is obtained by attempting to find the dependence that these attributes of the pattern have on the value of B_y .

This task was undertaken by utilizing the DE-2 data base of electrostatic potential distributions derived from each high latitude satellite pass (Hairston and Heelis, 1990). Fits to the data were performed to determine the location of the zero crossing for extreme values of positive and negative B_y . The results are shown in figure 3. Similarly the data can be examined for changes in the local time distribution of the potential around the convection reversal boundary (Lu et al., 1989). In addition to changes in the geometry of the convection cells as a function of the IMF B_y component, it is also found that the absolute value of the potential extrema on the boundary are dependent on this parameter. Figure



P_{max} 30 P_{min} -40
 f -5.0 B_y 0.0

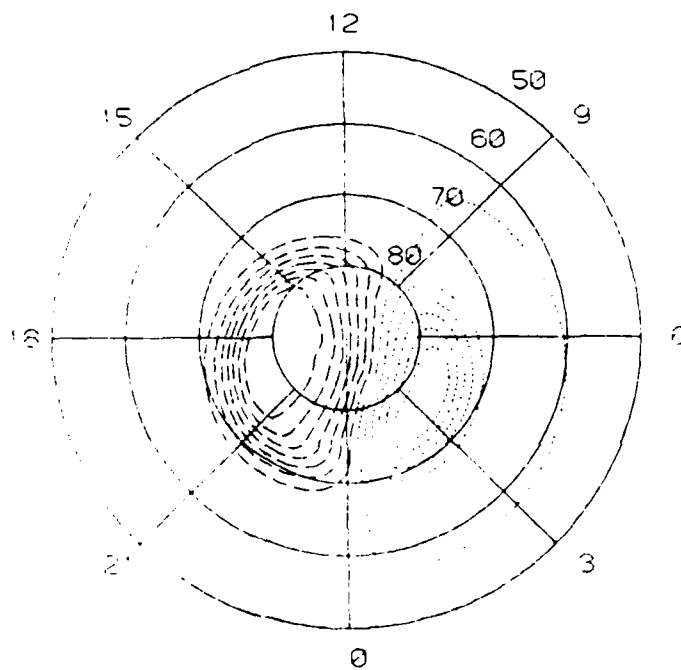
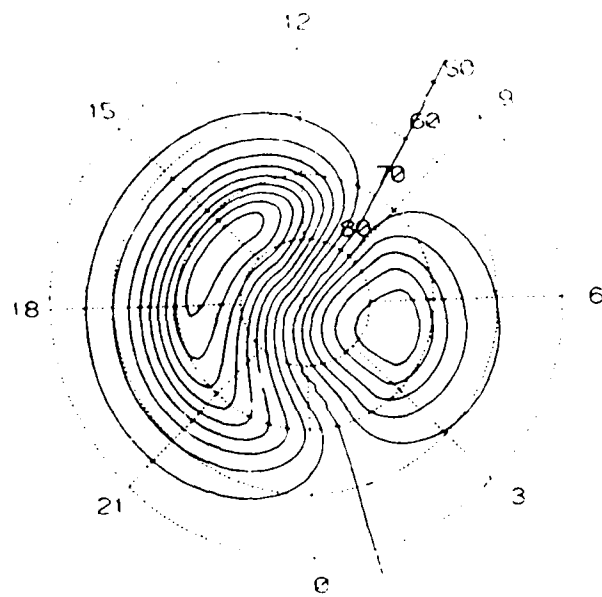


Figure 1. High Latitude Convection Pattern constructed from Latitude and Local Time distributions.

$\text{P}_{\text{simax}} = 29 \text{ Kv}$ $\text{P}_{\text{simin}} = 47 \text{ Kv}$

$r = -5.0$ $B_y = -7$



$\text{P}_{\text{simax}} = 33 \text{ Kv}$ $\text{P}_{\text{simin}} = 47 \text{ Kv}$

$r = -5.0$ $B_y = +8$

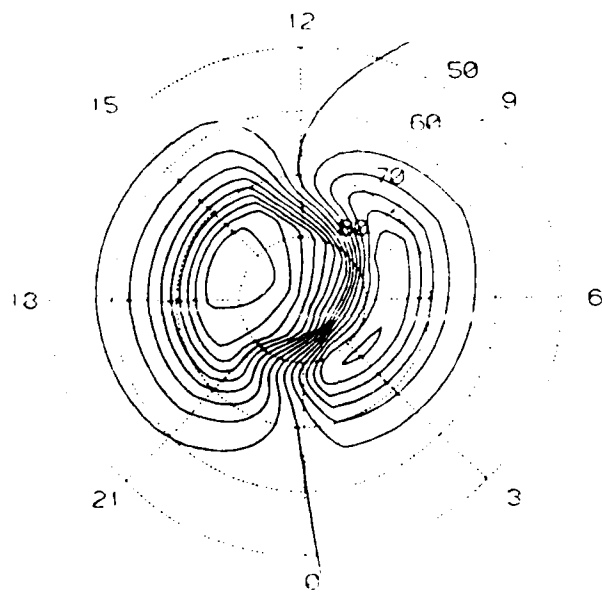


Figure 2. Representations of IMF B_y dependence of Convection Patterns.

4 shows that while a significant scatter in the data exists, a trend toward a dependence on B_z can easily be discerned. Finally it is found that a dependence of the radius of the convection reversal boundary on the potential drop across it (Siscoe, 1982) can be confirmed. With this cumulative information it is possible to insert analytical dependences on B_z into the expressions describing the convection pattern and thus produce a model that is dependent only on the IMF magnitude and direction. The model produced to describe the convection pattern for southward IMF has two important attributes. First it allows a global pattern to be produced that displays the first order dependences on the IMF shown by observations. Second, it allows fundamental parameters of the model, such as the location and magnitude of the potential extrema, which can be directly derived from satellite data, to be input directly to the model. The model is thus capable of producing a global representation of the convection pattern, that directly reproduces data from a given satellite pass. This exercise can be done quickly and easily for a single pass, and the task now remains to make it adaptive to multiple data sets. Several improvements to the model require further study of the data.

At present we have a good representation of the potential distribution as a function of latitude in the polar cap region. However, the local time distribution around the polar cap boundary, and the latitude distribution for latitudes below the polar cap boundary is not well quantified. Larger data bases are required to advance our understanding of the potential distribution around the boundary. However, the distribution at latitudes below the polar cap boundary requires us first to understand the geophysical variables that control its behavior. It is clear that during magnetic storms the magnetospheric field penetrates to lower latitudes in the ionosphere, but the temporal and spatial dependence of the phenomena is not well established. This present model is useful in determining the convective history of ionospheric plasma and the effects that changes in the pattern might have on observed plasma distributions at high latitudes.

2.1.2. Northward IMF

One of the products of the convection model development for southward IMF is the capability to produce a single convection cell of almost arbitrary shape and representing either clockwise or anticlockwise circulation. With this capability it is possible to begin development of a representation of the convection pattern for northward IMF by assuming that the pattern can be represented by four circulation cells with shapes, potential distributions and locations that depend on the magnitude and orientation of the IMF. The problem is approached in a similar manner as the case for southward IMF. First we establish the capability to reproduce various configurations of the convection pattern

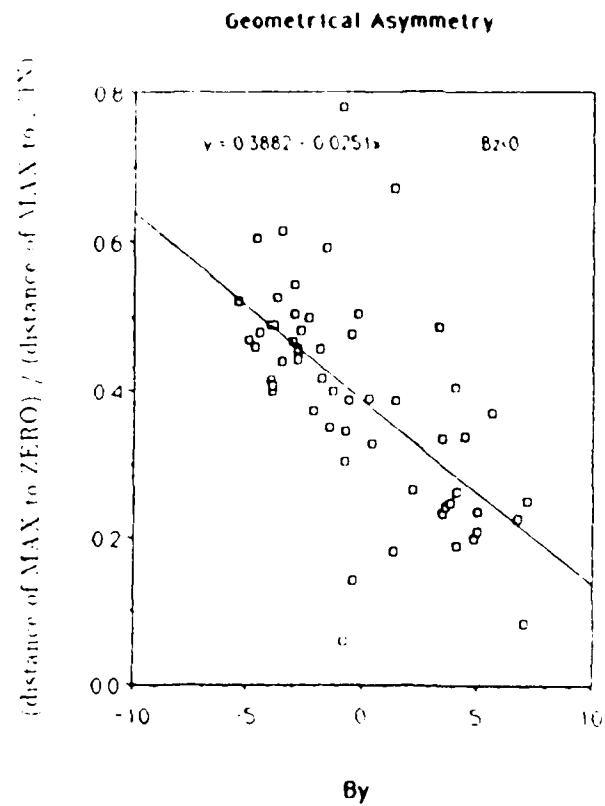


Figure 3. Dependence of geometrical asymmetry on IMF B_y .

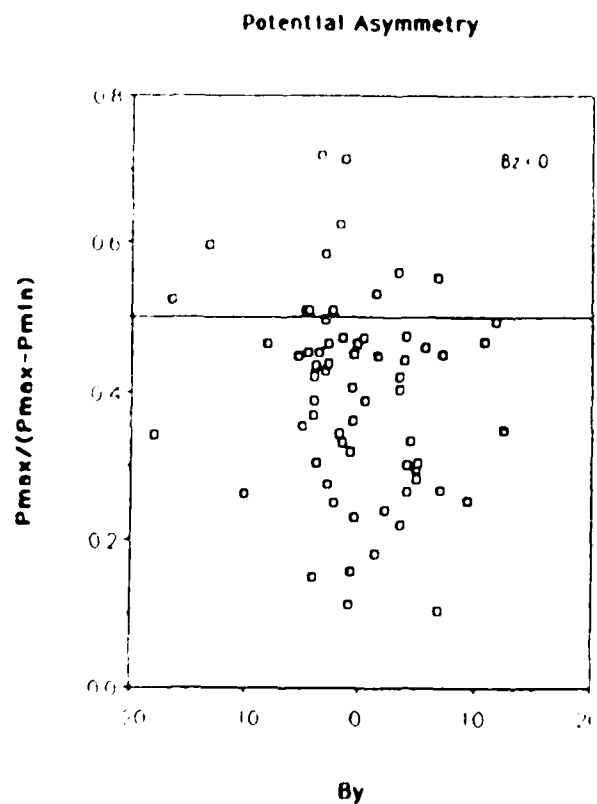


Figure 4. Dependence of Potential Asymmetry on IMF B_y .

$$P_{\max} = 15 \quad P_{\min} = -15 \quad C_{\text{int}} = 3$$

$$r = -4.0 \quad B_y = 0$$

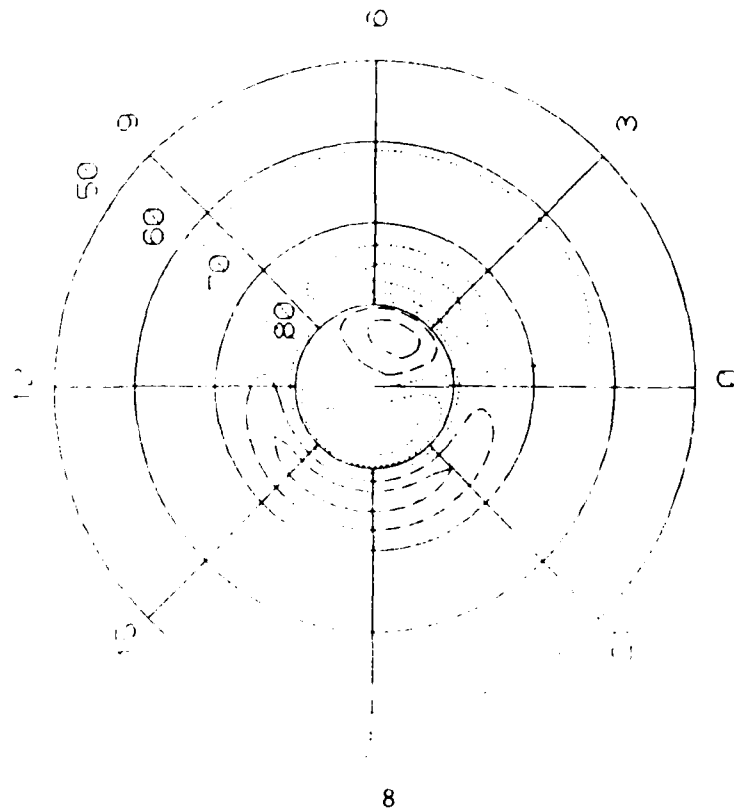


Figure 5a.

Symmetric four-cell convection pattern constructed for northward IMF.

$$P_{\max} = 17 \quad P_{\min} = -15 \quad C_{\text{int}} = 3$$

$$r = -4.0 \quad B_y = 0$$

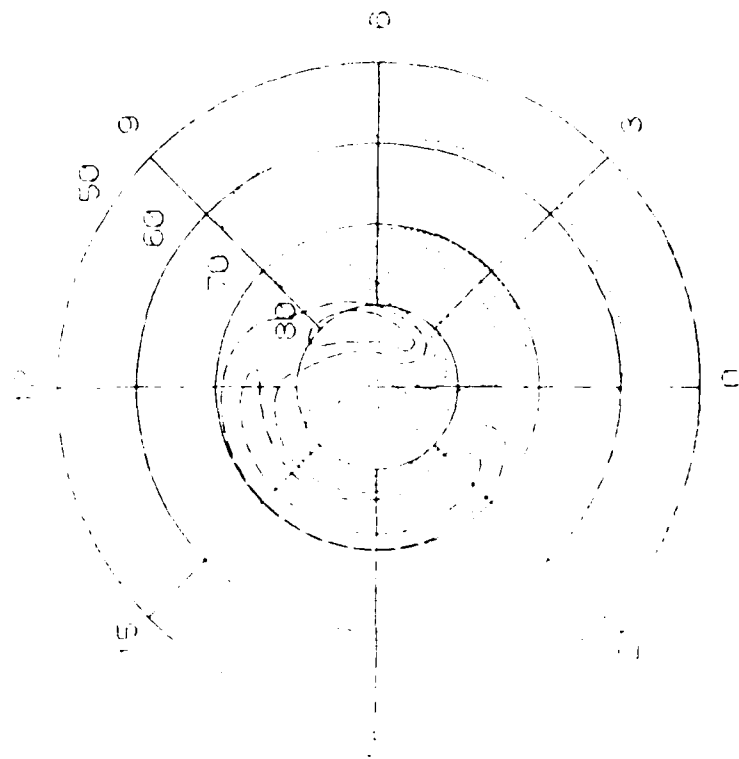


Figure 5b.

Distorted two-cell convection pattern constructed for northward IMF.

that have been put forward as representations for the flow during times of northward IMF. Then we determine the functional dependence of the controlling parameters on the IMF itself in order to arrive at a mathematical model. To date, the capability to reproduce many representations of the convection pattern has been established. Two extremes are a four-cell configuration put forward by a number of researchers (e.g. Burke et al., 1979, Maezawa, 1976) and a distorted two-cell pattern described by others (e.g. Heppner and Maynard, 1987). The development of the convection model for northward IMF assumes the existence of two drivers for the convective motion. One, that we will term "viscous interaction" is assumed to be derived from an electric field in the magnetospheric low-latitude boundary layer and is independent of the IMF but not of the solar wind speed and density. It produces an essentially symmetric two-cell convection pattern in the ionosphere, although as stated previously the dependences of the parameters in the model on external conditions has not yet been established. The second driver is derived from direct connection between the IMF lines in the magnetosheath with the geomagnetic field. This electric field and resulting convection pattern in the ionosphere is dependent on the IMF magnitude and orientation as well as the solar wind speed and density. It produces the familiar asymmetries in the convection pattern that have been studied for the case of southward IMF and in fact dominates the convection pattern during such periods. During northward IMF, however, the relative importance of these two drivers is not yet established and they combine to produce the variety of representations of the convection pattern that have been put forward in the literature. Figure 5 shows the capabilities of the model constructed in this way. The top panel shows a four-cell pattern obtained by adding the two cell convection patterns from each driver. Here we have assumed that both drivers produce symmetric patterns and thus, the resulting configuration is somewhat idealistic. Nevertheless, it allows us to establish variables such as the location of the convection pattern center and the radius of the convection reversal boundary for each driver, upon which a more realistic pattern may be developed. If these parameters are change and a less symmetric potential distribution for the "direct connection" driver is assumed, then the second panel shows quite convincingly how a distorted two-cell pattern may be formed. In addition to providing the capability to reproduce such convective configurations, the formulations currently being examined allow some insight into the evolution of the convection pattern from one state to another.

The availability of a convection model that allows the separate specification of flow patterns from two sources, raises the issue of their relative importance. Here we must recognize the difficulty in identifying the different drivers from ionospheric measurements, due to our inability to unequivocally determine the magnetic field topology. In an attempt

to shed some light on this topic we have undertaken a statistical study of the relationships between the boundaries in energetic particle precipitation regions and the boundaries in the convection pattern that mark reversals in the ion drift from sunward to antisunward (Coley et al., 1987). It is found that the identification of antisunward flow within a region of auroral precipitation is subject to some uncertainty because the region of overlap is generally very small. Thus the signature of "viscous interaction" in the ionosphere is very small. Either it is similarly small at the magnetopause, and can account for only a small fraction of the total cross polar cap potential, or the existence of parallel potential drops between the source and the ionosphere make it impossible to determine the relative importance from ionospheric measurements. Examination of the data shows that both sunward and antisunward convection on open field lines may be a relatively frequent occurrence on the dayside of the dawn-dusk meridian, during times when the IMF B_y component is large. The data support the convective configuration proposed by Burch et al. (1985) in which both flow directions in the ionosphere are associated with flow in the lobes of the magnetotail. This "lobe cell" convection coexists with convection cells attributable to merging of the IMF with the Earth's closed field lines during times when the IMF is southward.

2.1.3. Temporal evolution of the Convection Pattern

In addition to attempts at constructing analytical expressions for the electrostatic potential distribution, the consequences of specifying the potential distribution around the convection reversal boundary and subsequently deriving the global potential from a solution of the Laplace equation have also been examined. A scenario is adopted for the solar wind/magnetosphere/ionosphere coupling where closed magnetospheric flux tubes merge with the solar wind magnetic field. The resulting opened field lines convect across the polar cap ionosphere because of field line tension (Moses et. al., 1988,1989). In the model, the ionospheric plasma is treated as a two-dimensional fluid. An adiaroic boundary that approximates the convection reversal is placed in the fluid (Siscoe and Huang, 1985). Gaps in the adiaroic boundary allow flux to enter and leave and the boundary expands or contracts at a rate determined by the potential distribution along it and the net magnetic flux into or out of the region enclosed by the reversal boundary. The potential across the gap and the orientation of the gap is chosen to best reproduce the properties of individual data sets examined for different orientations of the IMF. It can be shown that by appropriately locating the position of multiple gaps in the adiaroic line, a good representation of the convection pattern can be obtained. Figure 6 shows one such example in which a dayside and a nightside gap are required but where the flux entering and leaving the polar cap is not equal. Thus the polar cap expands. During active periods intense electric fields form

premidnight. Also, on average the dawn convection cell spreads and the dusk cell retreats premidnight. The nightside gap forms along a meridian between 2200 and 0200 MLT, presumably when reconnection is occurring in the tail. Results indicate that the nightside gap forms after the expansion phase onset of a substorm and remains open through the recovery phase.

The usefulness of this description of the convection pattern lies in a deeper understanding of the response of the ionospheric convection pattern to changes in the IMF and in response to substorm activity, shape of the convection reversal boundary and the distribution of potential. These findings should be incorporated into the next level of sophistication in analytical models.

2.2. Plasma Structures and convective flow

The appearance of plasma structures of varying scale sizes in the high latitude region, is of interest for many reasons. They are signatures of the temporal evolution of sources, sinks and transport of plasma in the region. They are also the seat of plasma density gradients subject to a variety of plasma instabilities. Here we confine our attention to the existence of so-called patches of ionization seen to convect antisunward across the polar cap during times of southward IMF [Weber et al., 1984]. These patches have scale sizes of 1000 km or so and measurements of the electron temperature inside them indicate that they are not the product of a local ionization source from precipitating particles. Other possible sources for plasma structure may be due to different residence times in regions where the plasma is produced. These regions lie in the auroral zone and the cusp. We have undertaken an initial study of the effects of a change in orientation of the convection pattern, due to changes in B_y , on the residence times of plasma packets in the auroral zone and cusp. Our hypothesis is that the boundary of a plasma enhancement in the polar cap marks a change in the convective history of the plasma. Initial studies [Anderson et. al., 1988], indicate that this could indeed be the case. For a given location at very high latitudes, two effects must be taken account of when examining the total ion concentration. One is the radius of the polar cap itself, which is in turn related to the potential drop across it [Hairston and Heelis, 1990]. The other is the sign of B_y , which effects the orientation of the convection cells. Both these parameters can affect the past history of the plasma seen, for example at Thule. Figure 7 shows the predicted temporal evolution of the peak F-region density seen at Thule for two different configurations of the polar cap boundary. In one case (100 Kv x 15°) the plasma seen at Thule in the late afternoon has convected through the evening side

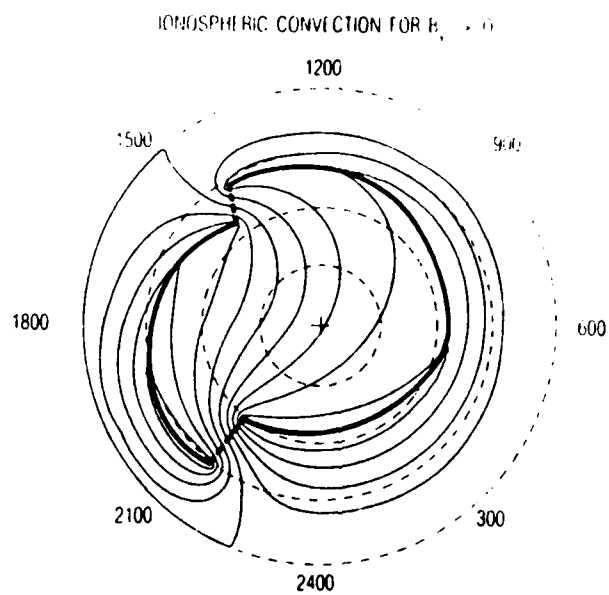
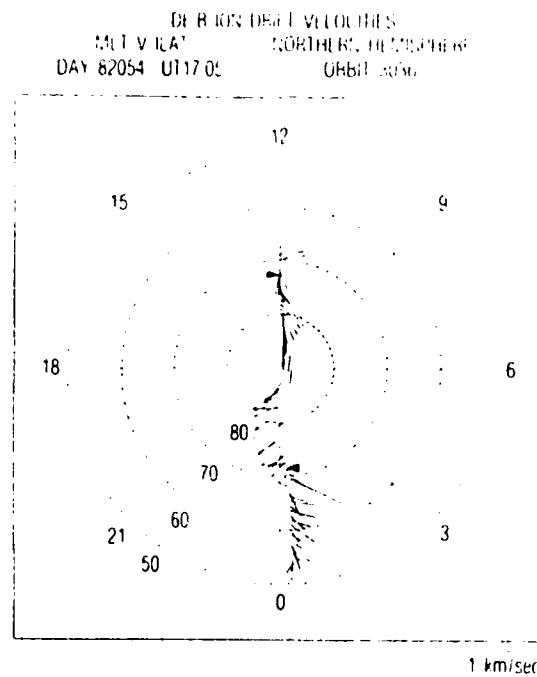


Figure 6. Representation of convective flow observed by DE-2 in terms of flow gaps in an adiabatic boundary.

auroral zone and spent a long time in solar illumination compared to the other case ($80 \text{ Kv} \times 12^\circ$) where at the same local time the plasma has convected from the morningside and spent little time in sunlight. It is clear that the different convective histories can produce the required differences in the total ion concentration. Further work is called for in this modelling effort to determine the effects of variations in the B_y component of the IMF and in the time scales for changes required to produce the plasma enhancements with spatial scales of a 1000 km or so.

2.3. Electrodynamics of Polar Cap Arcs.

In addition to the large scale convective features discussed previously, during periods of northward IMF, mesoscale features in the electric field and energetic particle environment pervade the entire high latitude region. On many occasions, these smaller scale features dominate the character of the plasma and are of considerable interest both electrostatically and morphologically in that they are indicators of a vastly different configuration of the magnetosphere during times of northward IMF from that existing during southward IMF. We have undertaken a study of the mesoscale features existing during times of northward IMF, by using a variety of satellite and ground based instrumentation. Our first task was to establish the electrodynamic configuration of the structures and subsequently to understand how they are related to the larger scale features of the auroral zone.

During times of northward IMF the existence of sun-aligned arcs at very high latitudes is well established [Lassen and Danielsen et al., 1978]. While observations from a satellite would suggest that the electric field configuration accompanying these arcs is somewhat turbulent and unorganized, a more complete examination from a variety of data sources serves to establish that this may not be the case [Carlson et al., 1988]. The uniqueness of our approach lies in the combination of one dimensional data from a polar orbiting satellite and two-dimensional imaging from the ground using all-sky cameras. This allows a detailed examination of the electrodynamics of polar cap arcs and also examination of the extent to which the features manifest themselves as coherent entities. Such studies have shown that polar cap arcs are frequently elongated in the noon-midnight direction. While they may be only a few hundred kilometers in the dawn-dusk dimension they may extend across the entire polar cap in the noon-midnight direction, being many thousands of kilometers in extent. Detailed examination of the electrodynamic properties of these arcs suggests that they may be associated with field-aligned potential differences. Figure 8 shows

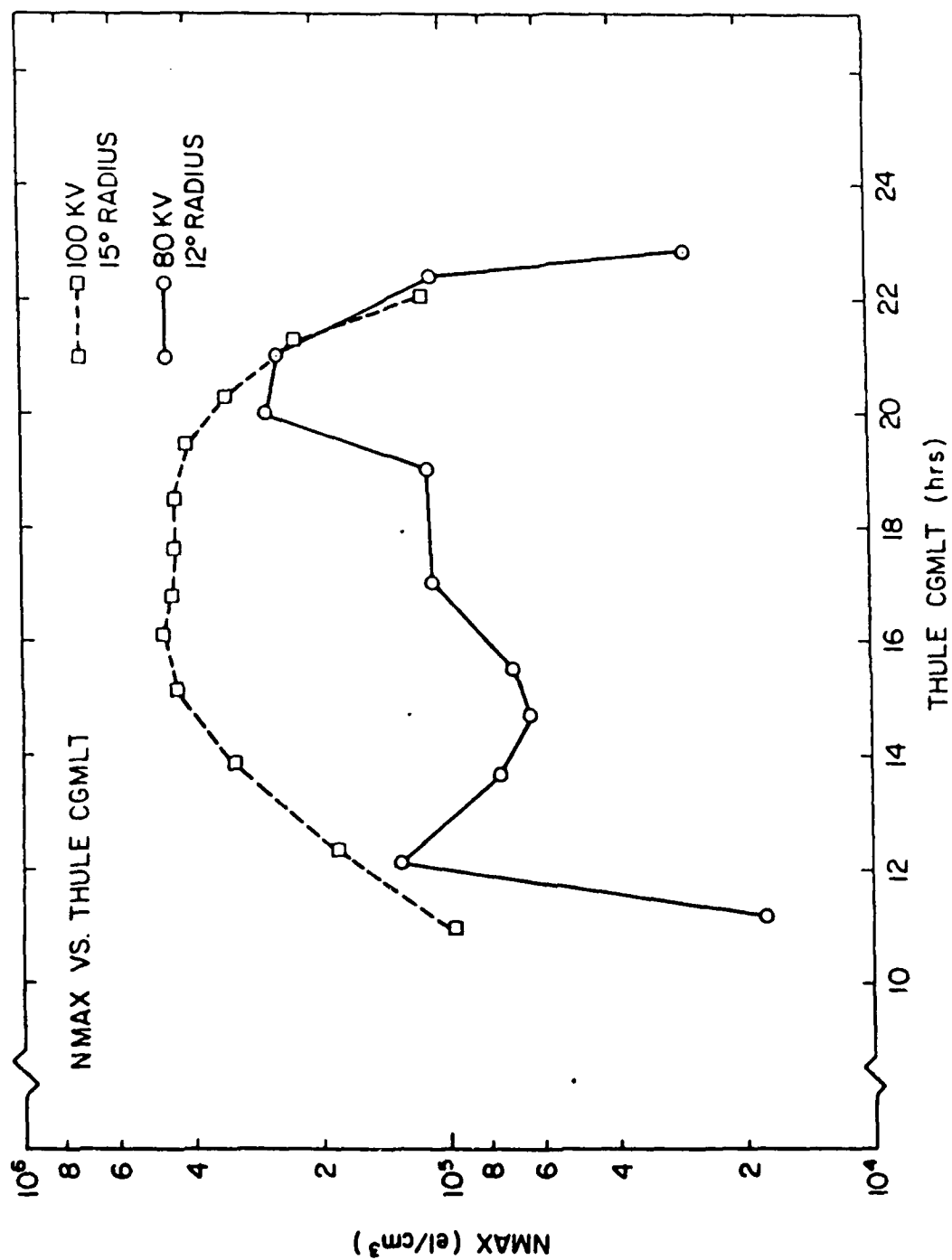


Figure 7. Calculated local time variation of F-peak concentration over Thule for different configurations of the convection pattern.

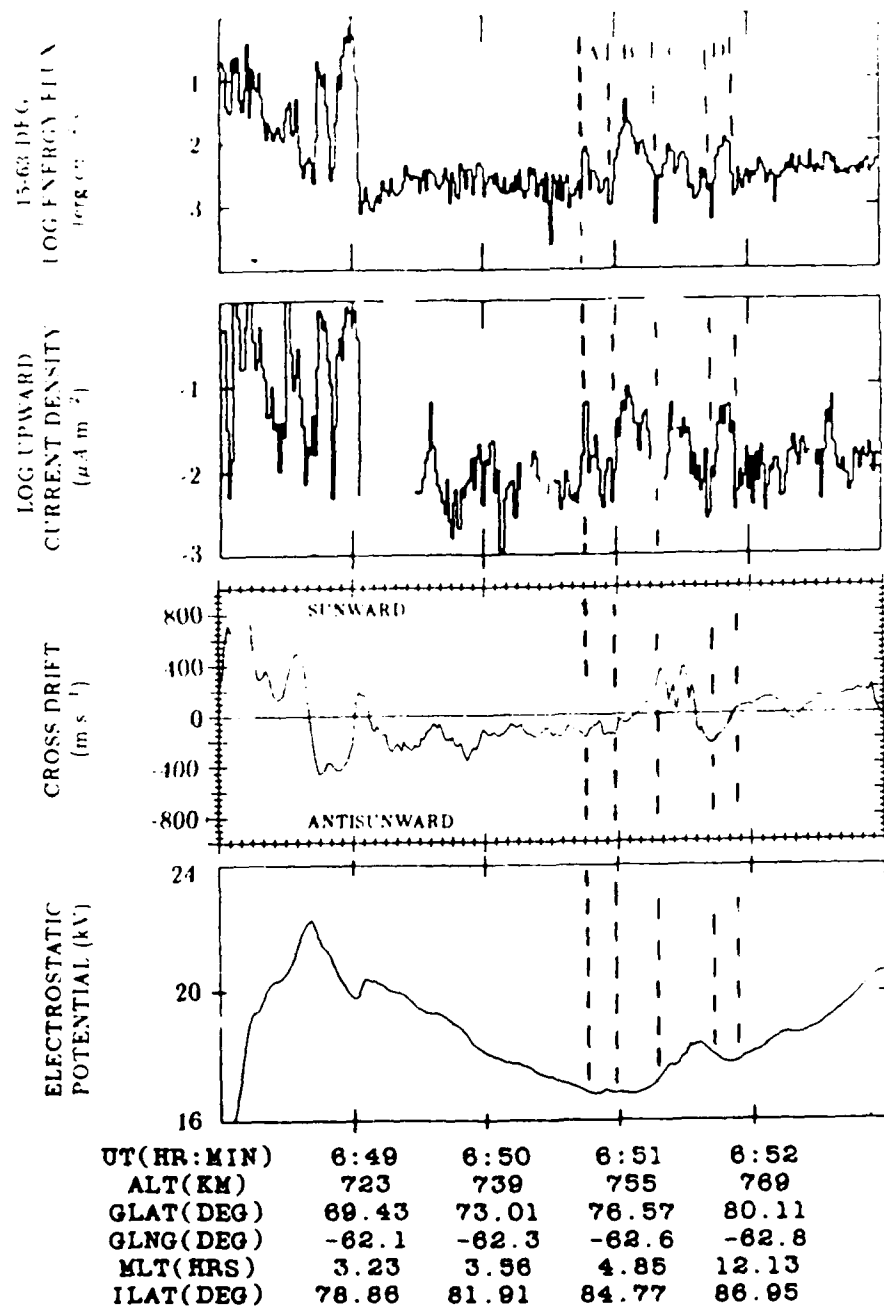


Figure 8. Electrodynamic properties observed by DE-2 during the crossing of four polar cap arcs.

DE-B ION DRIFT VELOCITIES
 MLT V ILAT
 DAY 82 21 UT 6:51
 NORTHERN HEMISPHERE
 ORBIT 2534

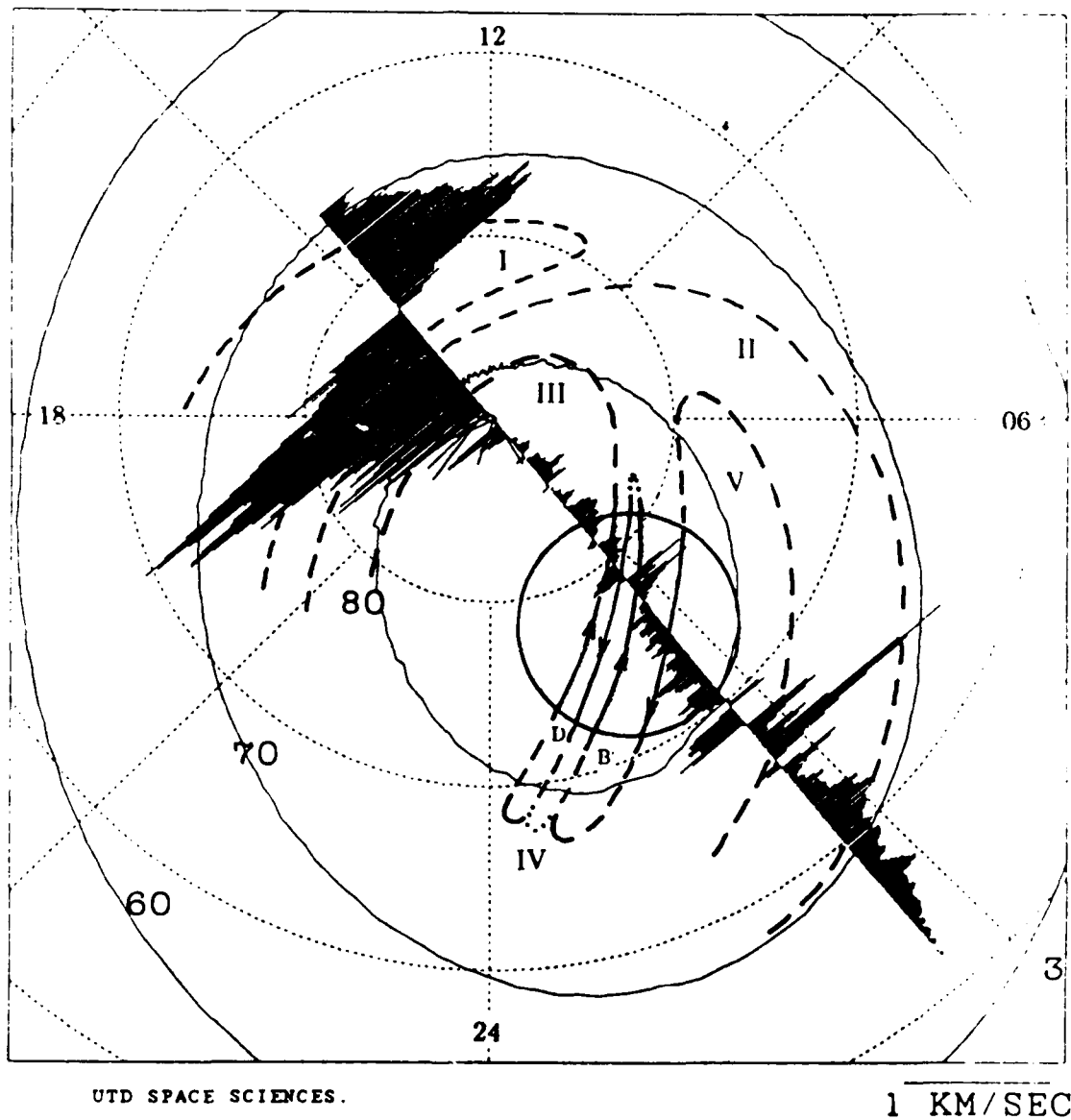


Figure 9. Mesoscale convection features identified with polar cap arcs and incorporated into a large scale global convection pattern.

the properties of four arcs, labelled A, B, C, and D. Each one is associated with a negative divergence in the electric field and in a uniform background conductivity would require an upward field-aligned current. Further examination of one of these arcs (B), shows that the precipitating electrons responsible for the emission are also carrying the required field-aligned current. Thus it appears that these arcs are electrodynamically similar to discrete arcs in the auroral zones [Lyons, 1981], but they apparently involve much smaller field aligned potential drops, since precipitating electrons with energies greater than 1 keV are rarely seen. The coherent nature of these arcs implies that their electrodynamic properties are similarly preserved along them. If this is the case then it is possible to construct possible mesoscale convection features associated with them. One such example is shown in figure 9. Here it is suggested that small scale "finger-like" convection cells exist around each discrete feature. Detailed observations are still required to determine the nature of the connection between these mesoscale features and the larger scale convection features associated with plasma flow through the auroral zone. A recent opportunity to observe such a feature in the nightside auroral zone using radar and satellite imagery has shown that the arc may denote the division between antisunward flow that rotates clockwise into the polar cap antisunward flow that rotates anticlockwise into the auroral zone [Nielsen et al., 1990]. Previous observations of the theta aurora [Frank et al., 1986], have suggested that the sunward flowing plasma is associated with closed field lines that presumably map to the central plasma sheet. The implication is that antisunward flow is associated with open field lines on either side of the transpolar arc. We note that this need not be the case and that the antisunward flow on one side of the arc may be associated with the low latitude boundary layer. Further work on the association between the global flow configuration and the appearance of sun-aligned arcs is necessary to advance our understanding of these features.

2.4. Electrical Coupling in Ionospheric Structures.

Studies of plasma structure in the high latitude ionosphere are complicated by the variety of structuring mechanisms and by the effects of transport, that can deliver structured plasma to places that are significant distances from the source. A previous section included some work and discussion about the formation of large scale structure from variations in the convective flow pattern. Here we are interested in the behavior of smaller scale structure as it is transported from its source. The electric field responsible for the transport will generally be of scale sizes larger than a few tens of kilometers and

originate from outside the ionosphere. However, the plasma structure itself will produce electric fields from the existence of pressure gradients, and these will exist at the variety of scale-sizes possessed by the structure. For scales sizes greater than about 5km the electric field associated with an isolated structure will map almost unattenuated along the magnetic field lines and its evolution will therefore depend on conditions existing at locations remote from the structure. For example, if an F-region structure convects over a highly conducting E-region, the electric field can be effectively shorted, thus increasing the rate at which this scale-size will decay if the E-region were not present. At scale sizes less than a few kilometers, this simple view of the processes acting to determine the evolution of F-region plasma structure is complicated by the fact that the magnetic field lines cannot be regarded as electric equipotentials. We have examined the processes involved utilizing two approaches. The first examines only the effects of the E-region on the temporal evolution of a plasma structure in the F-region. For this purpose we may assume that the F-region and E-region are slabs of plasma of some specified vertical extent, between which electric fields map and are unattenuated in so doing (Heelis et al., 1985). This simply means that an F-region structure will produce pressure gradient electric fields that may be partially shorted out by a conducting E-region. If the E-region is highly conducting then the F-region pressure gradient field will be shorted out and the structure will decay at a rate determined principally by the local perpendicular ion diffusion rate. If the E-region were a perfect insulator then the pressure gradient field would not be shorted and the plasma structure will decay at the local perpendicular electron diffusion rate. The real situation is, of course, in between these extremes, where the conducting properties of the E-region are important. However, as soon as the partially conducting E-region is considered, the effects of the E-region field on the local redistribution of plasma must be taken into account. This electric field tends to produce an image, in the E-region, of the F-region plasma structure.

The second approach considers in more detail the mapping properties of the electric field. In particular, it is important to understand that the electric field mapping process is scale size dependent (Heelis and Vickrey, 1990). Thus electric fields from F-region structures of small scale size (≤ 1 km) may be quite large but not map effectively to a highly conducting E-region. Electric fields from larger scale features in the F-region, map effectively to the E-region, but the electric fields are of smaller magnitude. In order to understand all these effects it is necessary to consider the altitude distribution of the electric field and the plasma. With this consideration we see that a given altitude below the source region for the electric field will show a preferred scale size at which the compressional effects (and therefore image formation) are a maximum. Since the electric field is proportional to

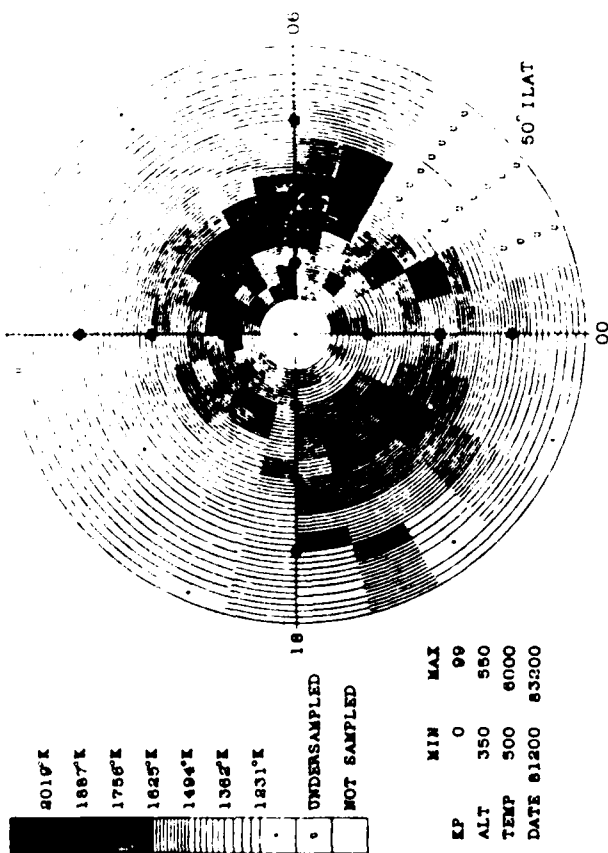
the plasma pressure gradient, electric fields are largest for smallest scale sizes at the source. However the smaller scale sizes do not map effectively away from the source. Thus the electric field at any location will be a combination of the altitude mapping process and the scale size under consideration. At large scale sizes, the amplitude of image structure will increase with decreasing scale sizes for all source perturbations whose amplitudes decrease less rapidly than k^{-2} . The inclusion of the electric field mapping process simply enforces a decrease in the amplitude of image structure at large k for any amplitude distribution of the source. Thus a high frequency "roll-off" of the image spectrum will always occur and will occur at smaller k values (larger scale-size) than predicted by a theory that does not include the electric field mapping properties.

3. Ionospheric Frictional Heating.

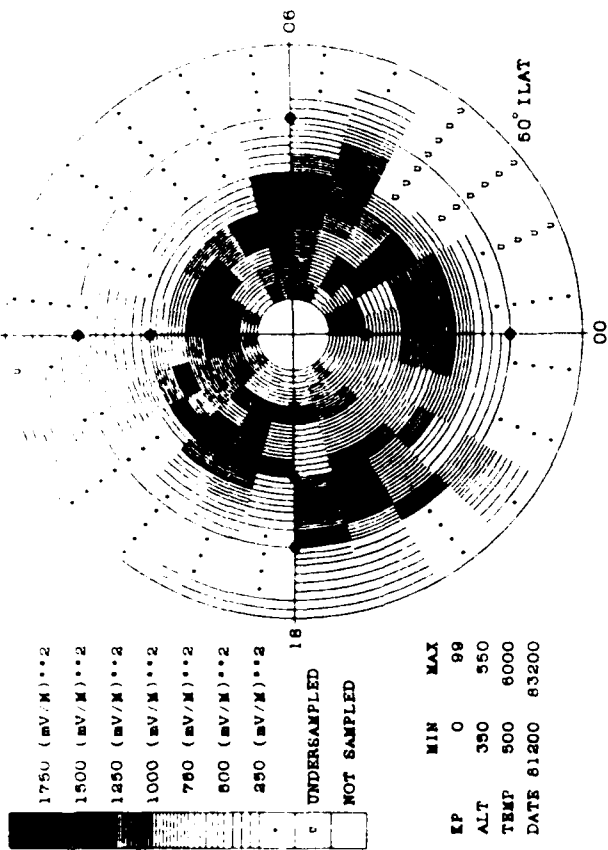
In addition to the importance in determining the convective history of the high latitude plasma and the response of the convection pattern to changes in the IMF, we are also interested in the effects of the plasma motion on its energy content. The large convective flow velocities seen at high latitudes, imply the existence of significant frictional heating, and in such areas, the plasma will expand, the plasma composition will change and the heat will be delivered to the neutral gas. In describing the effects of the plasma motion on the temperature of the gas it is important to distinguish between a heating rate determined from the product of the electric field and the height integrated Pedersen conductivity and the heating per particle determined from the local difference between the ion and neutral wind velocities. In order to understand the different implications of these two parameters we have undertaken a morphological study of the global distribution of the ion temperature and the ion velocity (Heelis and Coley, 1988). By examining the differences in the distributions of temperature and velocity we can ascertain the effects of local neutral winds in moderating or increasing the ion heating rate. By examining differences between the ion temperature distribution and the global frictional heating rate or $\Sigma_p E^2$, we can see the effects of the ion concentration on the ion temperature. Significant differences can be seen. Figure 10 serves to illustrate most of the features. The Joule heating rate is dependent on both the relative ion-neutral velocity and the total ion concentration. On the other hand, enhancements in the ion temperature depend only on the relative ion-neutral velocity. It is thus the heating rate per particle that is related to the ion temperature. Regions of large Joule heating rate produced by enhancements in the ion concentration will not necessarily be accompanied by enhancements in the ion temperature. In the F-region,

this phenomenon manifests itself in the cusp region. In the dawnside F-region, a local maximum in the ion temperature is seen in the F-region while no such maximum exists in the heating rate. In this case, a maximum in the ion neutral velocity certainly does exist, but this is counteracted by a minimum in the total ion concentration. Thus the heating rate per particle is a maximum, while the total heating rate is not.

AVERAGE ION TEMPERATURE
NORTHERN HEMISPHERE



AVERAGE EPERP*2
NORTHERN HEMISPHERE



AVERAGE RHO*(V1**2)
NORTHERN HEMISPHERE

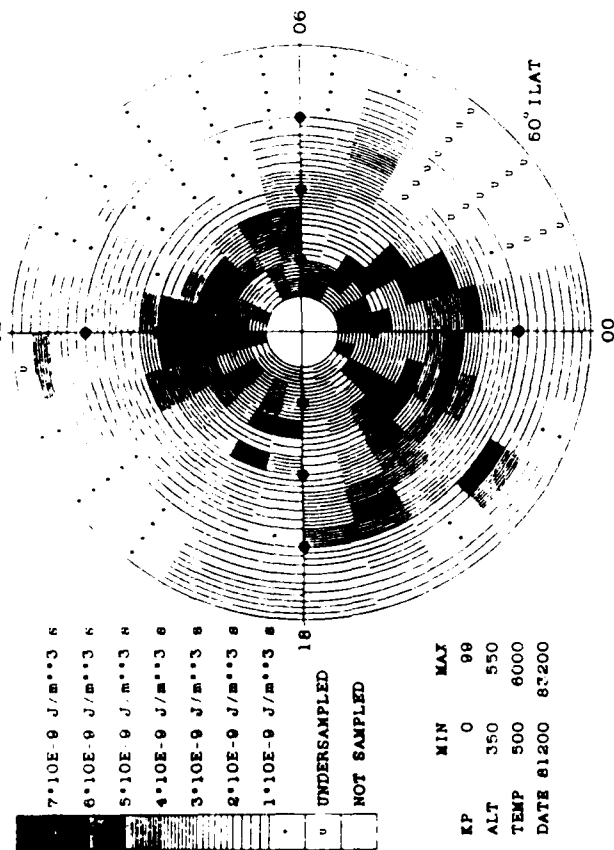


Figure 10. Global distributions of F-region ion temperature, ion velocity and frictional heating rate determined from DE-2.

References

- Anderson, D.N., J. Buchau, and R.A. Heelis, Origin of density enhancements in the winter polar cap ionosphere, *Radio Sci.*, **23**, 513, 1988.
- Burch, J.L., P.H. Reiff, J.D. Menietti, R.A. Heelis, W.B. Hanson, S.D. Shawhan, E.G. Shelley, M. Sugiura, D.R. Weimer, and J.D. Winningham, IMF B_y -dependent plasma flow and Birkeland currents in the dayside magnetosphere, 1, Dynamics Explorer observations, *J. Geophys. Res.*, **90**, 1577-1593, 1985.
- Burke, W.J., M.C. Kelley, R.C. Sagalyn, M. Smiddy, and S.T. Lai, Polar cap electric field structures with a northward interplanetary magnetic field, *Geophys. Res. Lett.*, **6**, 21, 1979.
- Carlson, H.C., R.A. Heelis, E.J. Weber, and J.R. Sharber, Coherent mesoscale convection patterns during northward interplanetary magnetic field, *J. Geophys. Res.*, **93**, 14501-14514, 1988.
- Coley, W.R., R.A. Heelis, W.B. Hanson, P.H. Reiff, J.R. Sharber, and J.D. Winningham, Ionospheric convection signatures and magnetic field topology, *J. Geophys. Res.*, **92**, 12352-12364, 1987.
- Frank, L.A., J.D. Craven, D.A. Gurnett, S.D. Shawhan, D.R. Weimer, J.L. Burch, J.D. Winningham, C.R. Chappell, J.H. Waite, R.A. Heelis, N.C. Maynard, M. Sugiura, W.K. Peterson, and E.G. Shelley, The Theta Aurora, *J. Geophys. Res.*, **91**, 3177-3224, 1986.
- Hairston, M.R., and R.A. Heelis, A model of the ionospheric convection pattern for southward IMF based on DE-2 observations, *J. Geophys. Res.*, in press, 1990.
- Heelis, R.A., and W.R. Coley, Global and local Joule heating effects seen by DE-2, *J. Geophys. Res.*, **93**, 7551, 1988.
- Heelis, R.A., J.F. Vickrey, and N.B. Walker, Electrical coupling effects on the temporal evolution of F-layer plasma structure, *J. Geophys. Res.*, **90**, 437, 1985.
- Heelis, R.A., and J.F. Vickrey, Magnetic field-aligned coupling effects on ionospheric plasma structure, *J. Geophys. Res.*, in press, 1990.
- Hepner, J.P., and N.C. Maynard, Empirical high latitude electric field models, *J. Geophys. Res.*, **92**, 4467-4489, 1987.
- Lassen, K., and C. Danielson, Quiet time pattern of auroral arcs for different directions of the interplanetary magnetic field in the Y-Z plane, *J. Geophys. Res.*, **83**, 5277-5283, 1978.
- Lockwood, M., and S.W.H. Cowley, Observations at the magnetopause and in the auroral ionosphere of momentum transfer from the solar wind, *Adv. Space Res.*, **8**, 281-299, 1988.
- Lu, G., P.H. Reiff, M.R. Hairston, R.A. Heelis, and J.L. Karty, Distribution of convection

- potential around the polar cap boundary as a function of the interplanetary magnetic field, *J. Geophys. Res.*, **94**, 13447-13461, 1989.
- Evans, L.R. Discrete aurora as the direct result of an inferred high altitude generating potential distribution, *J. Geophys. Res.*, **86**, 1, 1981.
- Maezawa, K., Magnetospheric convection induced by the positive and negative Z components of the interplanetary magnetic field: Quantitative analysis using polar cap magnetic records, *J. Geophys. Res.*, **81**, 2289-2303, 1976.
- Moses, J.J., G.L. Siscoe, R.A. Heelis, and J.D. Winningham, A model for multiple throat structures in the polar cap flow entry region, *J. Geophys. Res.*, **93**, 5741-5759, 1988.
- Moses, J.J., G.L. Siscoe, R.A. Heelis, and J.D. Winningham, Polar cap deflation during magnetospheric substorms, *J. Geophys. Res.*, **94**, 3785-3789, 1989.
- Nielsen, E., J.D. Craven, L.A. Frank, and R.A. Heelis, Ionospheric flows associated with a transpolar arc, *J. Geophys. Res.*, submitted, 1990.
- Siscoe, G.L., and T.S. Huang, Polar cap inflation and deflation, *J. Geophys. Res.*, **90**, 543-547, 1985.
- Siscoe, G.L., Polar cap size and potential: A predicted relationship, *Geophys. Res. Lett.*, **9**, 642-675, 1982.
- Weber, E.J., J. Buchau, J.G. Moore, J.R. Sharber, R.C. Livingston, J.D. Winningham, and B.W. Reinisch, F-layer ionization patches in the polar cap, *J. Geophys. Res.*, **89**, 1683-1696, 1984.

4. Publications.

The previously described research effort has provided is the opportunity, not only to study and advance our understanding of the dynamics and composition of the high-latitude ionospheric plasma, but also to distribute the results to the community in publications. While this report attempts to summarize the findings of our work, it is more completely described in 9 publications that have appeared or will shortly appear in the literature. The following pages contain abstracts of preprints or reprints from the published papers:

- Coley, W.R., R.A. Heelis, W.B. Hanson, P.H. Reiff, J.R. Sharber, and J.D. Winningham, Ionospheric convection signatures and magnetic field topology, *J. Geophys. Res.*, **92**, 12352-12364, 1987.
- Heelis, R.A., and W.R. Coley, Global and local Joule heating effects seen by DE-2., *J. Geophys. Res.*, **93**, 7551, 1988.
- Anderson, D.N., J. Buchau, and R.A. Heelis, Origin of density enhancements in the winter polar cap ionosphere, *Radio Sci.*, **23**, 513, 1988.
- Moses, J.J., G.L. Siscoe, R.A. Heelis, and J.D. Winningham, A model for multiple throat structures in the polar cap flow entry region, *J. Geophys. Res.*, **93**, 5741-5759, 1988.
- Carlson, H.C., R.A. Heelis, E.J. Weber, and J.R. Sharber, Coherent mesoscale convection patterns during northward interplanetary magnetic field, *J. Geophys. Res.*, **93**, 14501-14514, 1988.
- Moses, J.J., G.L. Siscoe, R.A. Heelis, and J.D. Winningham, Polar cap deflation during magnetospheric substorms, *J. Geophys. Res.*, **94**, 3785-3789, 1989.
- Hairston, M.R., and R.A. Heelis, A model of the ionospheric convection pattern for southward IMF based on DE-2 observations, *J. Geophys. Res.*, , in press, 1990.
- Nielsen, E. J.D. Craven, L.A. Frank, and R.A. Heelis, Ionospheric flows associated with a transpolar arc, *J. Geophys. Res.*, submitted, 1990.
- Heelis, R.A., and J.F. Vickrey, Magnetic field-aligned coupling effects on ionospheric plasma structure., *J. Geophys. Res.*, in press, 1990.

Ionospheric Convection Signatures and Magnetic Field Topology

W. R. COLEY, R. A. HEELIS, AND W. B. HANSON

Center for Space Sciences, University of Texas at Dallas, Richardson, Texas

P. H. REIFF

Center for Space Physics, Rice University, Houston, Texas

J. R. SHARBER AND J. D. WINNINGHAM

Southwest Research Institute, San Antonio, Texas

We present here a statistical study of signatures of the high-latitude ionospheric convection pattern and the simultaneously observed energetic electron precipitation. We most often find convection cells in which the sunward flowing region contains auroral particle precipitation but the antisunward flowing region does not. However, our observations also show the frequent occurrence of convection cells in which neither the antisunward nor the sunward flowing plasma region contains auroral particle precipitation. These findings may appear within the dawnside or duskside convection pattern and strongly suggest that such convection cells may be associated with open magnetic field lines that thread the magnetotail lobes. Examination of the interplanetary magnetic field (IMF) data shows that this "lobe cell" convection signature is most likely to be accompanied by the signature of dayside merging when the IMF has a significant y component but is directed southward. A lobe convection cell has a location and sense of circulation that are dependent on the sign of B_y . For the northern hemisphere, clockwise circulation displaced to the duskside appears roughly 35% of the time when B_y is positive, and anticlockwise circulation displaced to the dawnside appears when B_y is negative. The same circulation sense and location exist in the southern hemisphere for the opposite polarity of B_y . At times of northward IMF, the circulation within the polar cap can be at least partially on closed field lines and cannot be easily reconciled with merely a distortion of the standard "two-cell" convection pattern. The significance of these results to several models of the solar wind/magnetosphere interaction is discussed.

Global and Local Joule Heating Effects Seen by DE 2

R. A. HEELIS AND W. R. COLEY

Center for Space Sciences, University of Texas at Dallas, Richardson

In the altitude region between 350 and 550 km, variations in the ion temperature principally reflect similar variations in the local frictional heating produced by a velocity difference between the ions and the neutrals. Here we show the distribution of the ion temperature in this altitude region and discuss its attributes in relation to previous work on local Joule heating rates. In addition to the ion temperature, instrumentation on the DE 2 satellite also provides a measure of the ion velocity vector representative of the total electric field. From this information we derive the local Joule heating rate. From an estimate of the height-integrated Pedersen conductivity it is also possible to estimate the global (height-integrated) Joule heating rate. Here we describe the differences and relationships between these various parameters.

Origin of density enhancements in the winter polar cap ionosphere

D. N. Anderson and J. Buchau

Air Force Geophysics Laboratory, Hanscom Air Force Base, Massachusetts

R. A. Heelis

University of Texas at Dallas, Richardson, Texas

(Received September 15, 1987; revised January 20, 1988; accepted January 26, 1988.)

Coherent and incoherent ground-based radar measurements of the winter polar cap ionosphere at Thule and Sondrestrom, Greenland have established the existence of "patches" of enhanced ionization which drift across the polar cap in an antisunward, noon-midnight direction. Associated with these patches is strong radio scintillation activity which severely disrupts ground-to-satellite communication systems and interferes with the operation of space surveillance radar at high latitudes. Several recent studies have shown that the source of enhanced ionization is the sunlit subcusp ionosphere rather than production by precipitating energetic particles. However, the question of what causes the patchiness has not been addressed. We study this problem by solving the time-dependent plasma continuity equation including production by solar ultraviolet radiation, loss through charge exchange, and transport by diffusion and convection $E \times B$ drifts. Time and spatially varying, horizontal $E \times B$ drift patterns are imposed, and subsequent ionospheric responses are calculated to determine how enhanced plasma densities in the dark polar cap could result from extended transit of relevant flux tubes through regions of significant solar production. This would occur south of the cusp prior to convection as patches across the polar cap. It is found that a density enhancement in N_{max} from 7×10^6 to 5×10^7 el cm⁻³ occurs at Thule when a time-varying convection pattern is included in the simulation. The patch of ionization is generated when an initial convection pattern characterized by an 80-kV cross-tail potential and a 12° polar cap radius is abruptly changed to a 100-kV cross-tail potential and a 15° polar cap radius. The horizontal extent of the patch is related to the length of time the new convection pattern remains "turned on."

JOURNAL OF GEOPHYSICAL RESEARCH, VOL. 93, NO. A9, PAGES 9785-9790, SEPTEMBER 1, 1988

A Model for Multiple Throat Structures in the Polar Cap Flow Entry Region

J. J. MOSES,¹ G. L. SISCOE,² R. A. HEELIS,¹ AND J. D. WINNINGHAM⁴

A two-dimensional ionospheric convection model has been developed to produce convection patterns for southward interplanetary magnetic field (IMF) and a positive or negative IMF y component. The model consists of a movable, shear convection reversal boundary with a gap in it where flux enters the polar cap. The sign of IMF B_y determines the dayside gap geometry. We use this simple model to simulate measured ionospheric flows from the DE 2 satellite. Roughly 35% of DE 2 passes that cross the dayside between 0800 and 1400 hours MLT cannot be modeled with a single narrow flow entry region. By comparing model calculations and the measured ion flows, we show that the dayside flow entry region to the polar cap typically spans several hours in local time. The electric field can concentrate along portions of the polar cap entrance and weaken between the concentrated regions, thus forming multiple "throats."

COHERENT MESOSCALE CONVECTION PATTERNS DURING NORTHWARD INTERPLANETARY MAGNETIC FIELD

H. C. Carlson,¹ R. A. Heelis,² E. J. Weber,¹ and J. R. Sharber³

Abstract. All-sky imaging photometer (ASIP) and coincident DE 2 satellite plasma drift and particle data have been combined to study polar ionospheric convection in the presence of subvisual intensity, soft-particle excited (F region), 6300-Å, Sun-aligned polar cap arcs. Coincident DE-B drift meter data identify these arcs electrostatically as lines of negative electric field divergence. Based on conductivities, derived from the DE-B (low-altitude plasma instrument) measured particle fluxes, and the measured electric field gradients, the divergence of horizontal current across these particle impact excited arcs is in good quantitative agreement with upward Birkeland currents carried by the measured particle fluxes. Although velocity structure can be found without arcs, given the ASIP identified condition of stable weak (hundreds of rayleighs) 6300-Å Sun-aligned arcs in the polar cap, electric field negative divergence is consistently found. These arcs (of the order of 100 km in width) are found by ASIPs in the polar cap about half the time under $B_z > 0$ interplanetary magnetic field conditions. They are regularly seen by ASIP data to extend 1000 to over 2000 km in the sunward direction, and to persist in time often for over an hour. We are thus led to conclude that velocity gradients of this noon-midnight elongated scale are typical of $B_z > 0$ conditions. We further conclude that combined polar ASIP images and electrostatic potentials calculated along transpolar satellite tracks offer a valuable diagnostic for polar ionospheric convection studies under $B_z > 0$ conditions. The ASIP time continuous two dimensionality and the satellite equipotential scaling allow individual "snapshots" of these polar convection boundaries. Application here demonstrates highly anisotropic temporally stable convection with greater order than has previously been suspected.

Polar Cap Deflation During Magnetospheric Substorms

J. J. MOSES,¹ G. L. SISCO,² R. A. HEELIS,³ AND J. D. WINNINGHAM⁴

The expanding contracting polar cap model has been used to simulate DE 2 ion drift data during substorms as determined using the *AL* index. Of the 39 cases modeled, 57% required the opening of a nightside gap which maps to where reconnection occurs in the tail; 75% of the 16 recovery phase cases required a nightside gap while only 29% of the 17 expansion phase cases required a nightside gap. On the basis of this result, we conclude the following: If a nightside gap implies tail reconnection, then reconnection probably occurs after expansion phase onset and continues throughout most of the recovery phase of a substorm.

Model of the High-Latitude Ionospheric Convection Pattern During Southward Interplanetary Magnetic Field Using DE 2 Data

M. R. HAIRSTON AND R. A. HEELIS

Center for Space Sciences, University of Texas at Dallas, Richardson

Data from the polar-orbiting satellite DE 2 are used to calculate one-dimensional electrostatic potential distributions across the polar cap region. Using passes that lie within ± 3 hours MLT of the dawn-dusk line, various parameters of the polar potential distribution (location and magnitude of the maxima and minima, location of the zero potential point, etc.) are analyzed in relation to each other and to the interplanetary magnetic field (IMF). The resulting dependences are used to derive a two-dimensional model of the distribution of the electrostatic potential in the high-latitude ionosphere during times of southward IMF. This model can be generated using as inputs either the ionospheric potential parameters or, based on the relationships analyzed here, the IMF conditions. The capabilities of the resulting mathematical model are illustrated, and the importance of retaining a flexibility in the model to accommodate individual observations is emphasized.

Ionospheric Flows Associated With a Transpolar Arc

by

E. Nielsen¹, J.D. Craven², L.A. Frank² and R.A. Heelis³

¹ Max-Planck-Institut für Aeronomie,
Katlenburg-Lindau, FRG

² Department of Physics and Astronomy,

University of Iowa, Iowa City, Iowa, 52242 USA

³ University of Texas at Dallas, Richardson, Texas 75080 USA

Abstract

A theta aurora is observed in the northern hemisphere on 21 January 1982 using the auroral imaging instrumentation on board the DE-1 spacecraft. The period of observations is from 1807 to 2121 UT. The transpolar arc is observed to advanced toward the dusk sector, in the direction of the interplanetary magnetic field By component. Coincidentally, the intersection between the arc and the auroral oval near local midnight passes through the field-of-view of the STARE coherent radar system, thereby providing the opportunity for measurements of the spatial pattern of ionospheric electron drift velocities. The convection flow in the arc is directed toward the nightside auroral oval, where it divides into westward- and eastward-directed flows (eastward and westward electrojets). Sunward flows are not observed along the transpolar arc near midnight. The overall flow pattern is identical to that expected at the Harang discontinuity. Two traversals of the auroral oval and polar cap with DE 2 demonstrate that, as expected, transitions from antisunward to sunward flow are associated with the dayside of the transpolar arc. The evolution of the arc and its convective features observed simultaneously on both the dayside and the nightside allow a more complete description of its global configuration than has been made previously.

Magnetic Field-Aligned Coupling Effects on Ionospheric Plasma Structure

R. A. Heelis

The University of Texas at Dallas

J. F. Vickrey

SRI International

ABSTRACT

A mathematical description of the electrical coupling and dynamics of plasma structure in the E and F regions is presented. The scale size dependence of electric field coupling along the magnetic field is examined for a realistic background ionosphere and atmosphere. It is shown that, while normalized potentials map reciprocally between two altitudes, the potential disturbance caused by a fixed amplitude plasma density perturbation does not. The magnitude of the electrostatic potential created by structured ionization is also shown to be strongly dependent on the altitude of the structure.

The existence of plasma density structure at some altitude induces structure at other altitudes along the magnetic field in a scale size selective way. The early evolution of an F region structure that is initially confined in altitude is dominated by parallel diffusion. Low altitude image structure growth imposed by electrostatic fields mapped from the source is also very rapid; significant image amplitudes are reached in a matter of seconds. The altitude distribution of the evolving structure is strongly dependent on the scale size.

At E layer altitudes, where the Pedersen mobility is high and parallel diffusion relatively slow, a preferential scale-size for image structure is apparent for typical F region source spectra. This preferred scale size becomes smaller with increasing height. Above about 200 km altitude, however, parallel diffusion becomes increasingly important with height in determining the altitude and scale size distribution of structure resulting from a source at higher altitudes. The parallel diffusive flux can be modified by the existence of local plasma structure perpendicular to the magnetic field.